hp-DISCONTINUOUS GALERKIN METHOD FOR NONLINEAR PROBLEMS

Vít Dolejší

Charles University Prague
Faculty of Mathematics and Physics
Department of Numerical Mathematics
Sokolovská 83, 186 75 Praha, Czech Republic
dolejsi@karlin.mff.cuni.cz

Abstract

We deal with a numerical solution of nonlinear convection-diffusion problems with the aid of the discontinuous Galerkin finite element (DGFE) method. We propose a new *hp*-adaptation technique, which is based on a combination of a residuum-nonconformity estimator and a regularity indicator. The residuum-nonconformity estimator consists of two building blocks (the residuum error indicator and the value of the nonconformity). The estimator marks mesh elements for a refinement. The regularity indicator decides if the marked elements will be refined by *h*- or *p*-technique. The residuum-nonconformity estimator as well as the regularity indicator are easily computable quantities. Moreover, the same technique estimates an algebraic error arising from an iterative solution of the corresponding nonlinear algebraic system. The performance of the proposed *hp*-DGFE method is demonstrated by several numerical examples.

Keywords: *hp*-discontinuous Galerkin finite element method; residuum-nonconformity indicator; regularity estimator; algebraic error.

Introduction

Our aim is to develop a sufficiently robust, efficient and accurate numerical scheme for the simulation of viscous compressible flows. The *discontinuous Galerkin finite element* (DGFE) methods have become very popular numerical techniques for the solution of the compressible Navier-Stokes equations. Recent progress of the use of the DG method for compressible flow simulations can be found in [11].

In this paper, we deal with a model problem represented by a scalar nonlinear convection-diffusion equation. We focus on a *hp*-adaptation strategy of DGFE methods which significantly increase the accuracy and efficiency of the computation, see, e.g. [2, 6, 8, 12, 13].

The proposed strategy is based on a combination of a residuum-nonconformity estimator and a regularity indicator. The *residuum-nonconformity estimator* gives a lower estimate of the error measure consisting of the error measured in a dual norm and the quantity measuring a violation of the conformity of the solution. This estimator is locally defined for each mesh element, it is easily computable and its implementation is very simple. The *regularity indicator* is based on the integration of interelement jumps of the approximate solution over the element boundary. Taking into account results from a priori error analysis, we define the regularity indicator. If this value is smaller than one then we apply a *p*-refinement otherwise we use a *h*-refinement. Both refinements (*h* and *p*) are only isotropic, an anisotropic adaptation will be a subject of the further research.

1 Problem Formulation

1.1 Governing Equations

We consider a formal nonlinear *partial differential equation*

$$\begin{aligned} Lu &= 0 \quad \text{in } \Omega, && \text{(1a)}\\ u &= u_D \quad \text{on } \partial\Omega_D, && \text{(1b)}\\ Nu &= g_N \quad \text{on } \partial\Omega_N, && \text{(1c)} \end{aligned}$$

where $u : \Omega \to \mathbb{R}$ is the unknown scalar function defined on $\Omega \in \mathbb{R}^d$, $d = 2,3$, L is a formal second order differential operator and (1b) and (1c) formally represent the Dirichlet and Neumann boundary conditions on the parts of boundary $\partial\Omega_D$ and $\partial\Omega_N$, respectively. We assume that there exits a unique weak solution of (1) which we denote again by u.

Let $\mathscr{T}_h$ ($h > 0$) be a partition of the closure $\overline{\Omega}$ of the domain Ω into a finite number of closed d-dimensional simplicies K with mutually disjoint interiors. We call $\mathscr{T}_h = \{K\}_{K\in\mathscr{T}_h}$ a *triangulation* of Ω and do not require the conforming properties from the finite element method.

Over the triangulation $\mathscr{T}_h$ we define the so-called *broken Sobolev space*

$$H^s(\Omega,\mathscr{T}_h) := \{v; v|_K \in H^s(K)\ \forall K \in \mathscr{T}_h\}, \quad s \geq 0 \tag{2}$$

with the seminorm $|v|_{H^s(\Omega,\mathscr{T}_h)} := \left(\sum_{K\in\mathscr{T}_h} |v|^2_{H^s(K)}\right)^{1/2}$, where $|\cdot|_{H^s(K)}$ denotes the seminorm of the Sobolev space $H^s(K)$, $K \in \mathscr{T}_h$.

Moreover, to each $K \in \mathscr{T}_h$, we assign a positive integer p_K (=local polynomial degree). Then we define the set

$$\mathsf{p}_h := \{p_K, K \in \mathscr{T}_h\}. \tag{3}$$

We define the finite dimensional subspace of $H^1(\Omega,\mathscr{T}_h)$ which consists of discontinuous piecewise polynomial functions associated with the vector p_h by

$$S_{h\mathsf{p}} = \{v;\ v \in L^2(\Omega),\ v|_K \in P_{p_K}(K)\ \forall K \in \mathscr{T}_h\}, \tag{4}$$

where $P_{p_K}(K)$ denotes the space of all polynomials on K of degree $\leq p_K$, $K \in \mathscr{T}_h$.

We introduce a formal discretization of (1) with the aid of DGFE method. Hence, let

$$\tilde{c}_h(u,v) : H^2(\Omega,\mathscr{T}_h) \times H^2(\Omega,\mathscr{T}_h) \to \mathbb{R} \tag{5}$$

be the corresponding form which is nonlinear with respect to its first argument and linear with respect to the second one. We say that the function $u_h \in S_{h\mathsf{p}}$ is an *approximate solution* of (1), if

$$\tilde{c}_h(u_h, v_h) = 0 \qquad \forall v_h \in S_{h\mathsf{p}}. \tag{6}$$

Moreover, we define the form $\mathscr{N}_h : H^1(\Omega,\mathscr{T}_h) \to \mathbb{R}$ by

$$\mathscr{N}_h(v) := \left(2\sum_{\Gamma\in\mathscr{F}_h^I}\int_\Gamma h_\Gamma^{-1}[\![v]\!]^2\,\mathrm{d}S + \sum_{\Gamma\in\mathscr{F}_h^D}\int_\Gamma h_\Gamma^{-1}(v-u_D)^2\,\mathrm{d}S\right)^{1/2}, \tag{7}$$

where u_D is from (1b), $\mathscr{F}_h^I$ denotes the set of all interior faces of $\mathscr{T}_h$, $\mathscr{F}_h^D$ denotes the set of all faces of $\mathscr{T}_h$ lying on $\partial\Omega_D$, $[\![\cdot]\!]$ is the jump of a function from $H^1(\Omega,\mathscr{T}_h)$ and h_Γ is the diameter of a face Γ.

Finally, we characterise the weak solution of (1).

Lemma 1.1 *The following implications are valid:*

i) Let $u \in H^2(\Omega)$ *be the weak solution of* (1) *then*

$$\tilde{c}_h(u,v) = 0 \quad \forall v \in H^2(\Omega,\mathscr{T}_h), \tag{8a}$$
$$\mathscr{N}_h(u) = 0. \tag{8b}$$

ii) If $u \in H^2(\Omega,\mathscr{T}_h)$ *satisfies both conditions of* (8) *then u is the weak solution of* (1).

The discrete problem (6) represents a system of $N_h = \dim S_{h\mathsf{p}}$ nonlinear algebraic equations. We solve it with the aid of a Newton-like iterative method which gives the solution $\tilde{u}_h \in S_{h\mathsf{p}}$ such that $\tilde{c}_h(\tilde{u}_h, v_h) \approx 0 \; \forall v_h \in S_{h\mathsf{p}}$.

2 Residuum Estimator

In this section we investigate the discretization error $u - u_h$ and the algebraic error $\tilde{u}_h - u_h$ in a suitable (dual) norm and define estimators giving some information about these errors.

2.1 Error Measure

Similarly as in [3], our proposed error measure consists of *two building blocks*, which are motivated by Lemma 1.1, namely relations (8a) and (8b). Let $X := H^2(\Omega,\mathscr{T}_h)$ and $\|\cdot\|_X$ is a norm defined on X, which will be specified later. The *first building block* is given by

$$\mathscr{R}_h(u_h) := \sup_{0\neq v\in X} \frac{\tilde{c}_h(u_h,v)}{\|v\|_X} \tag{9}$$

which defines the *residuum error in the dual norm* of the approximate solution $u_h \in S_{h\mathsf{p}} \subset X$ and it measures a violation of (8a). However, it is impossible to evaluate $\mathscr{R}_h(u_h)$, since the supremum is taken over an infinite-dimensional space. Therefore, in our approach, we seek the maximum over some sufficiently large but finite dimension subspace of X, which is presented in Section 2.2.

The *second building block* is based on (8b), which characterises a violation of the conformity of the weak solution and a violation of the Dirichlet boundary condition. It is represented by the value $\mathscr{N}_h(u_h) \geq 0$ given by (7) which we call the *nonconformity* of the approximate solution. In contrast to $\mathscr{R}_h(u_h)$ the quantity $\mathscr{N}_h(u_h)$ is directly computable from (7). Finally, our *error measure* is the sum of squares of the *residuum error* and *nonconformity*, i.e.,

$$\mathscr{E}_h(u_h) := (\mathscr{R}_h(u_h)^2 + \mathscr{N}_h(u_h)^2)^{1/2}. \tag{10}$$

Due to Lemma 1.1 we simply observe that $\mathscr{E}_h(u_h) = 0$ if and only if $u_h = u$.

2.2 Global and Element Residuum Estimators

In the previous section, we introduced the error measure $\mathscr{E}_h(u_h) = \sqrt{\mathscr{R}_h(u_h)^2 + \mathscr{N}_h(u_h)^2}$ of the approximate solution $u_h \in S_{h\mathsf{p}} \subset X$. Whereas $\mathscr{N}_h(u_h)$ is easy to evaluate, the quantity $\mathscr{R}_h(u_h)$ has to be approximated in a suitable way, which is presented in this section. For each $K \in \mathscr{T}_h$ and each integer $p \geq 0$, we define the spaces

$$S_K^p := \{\phi_h \in X,\ \phi_h|_K \in P^p(K),\ \phi_h|_{\Omega\setminus K} = 0\} \tag{11}$$

and

$$S_{hp}^{+} := \{\phi \in X; \phi = \sum_{K \in \mathscr{T}_h} c_K \phi_K,\ c_K \in \mathbb{R},\ \phi_K \in S_K^{p_K+1},\ K \in \mathscr{T}_h\}. \tag{12}$$

Obviously, $S_{hp} \subset S_{hp}^{+} \subset X$.

Now, we define the *element residuum estimator*

$$\rho_{h,K}(u_h) := \sup_{0 \neq \psi_h \in S_K^{p_K+1}} \frac{\tilde{c}_h(u_h, \psi_h)}{\|\psi_h\|_X} = \sup_{\psi_h \in S_K^{p_K+1}, \|\psi_h\|_X = 1} \tilde{c}_h(u_h, \psi_h), \quad u_h \in X, \tag{13}$$

for each $K \in \mathscr{T}_h$ and the *global residuum estimator*

$$\rho_h(u_h) := \sup_{0 \neq \psi_h \in S_{hp}^{+}} \frac{\tilde{c}_h(u_h, \psi_h)}{\|\psi_h\|_X} = \sup_{\psi_h \in S_{hp}^{+}, \|\psi_h\|_X = 1} \tilde{c}_h(u_h, \psi_h), \quad u_h \in X, \tag{14}$$

which are easily computable quantities if $\|\cdot\|_X$ is suitably chosen, see Section 2.4.

Obviously, if $u \in X$ is the exact solution of (1) then consistency (8a) implies $0 = \rho_h(u) = \rho_{h,K}(u)$, $K \in \mathscr{T}_h$. Moreover, we have immediately a lower bound

$$\rho_h(u_h) \leq \mathscr{R}_h(u_h), \tag{15}$$

since ρ_h is the supremum over subspace $S_{hp}^{+} \subset X$. However, it is open if there exists an upper bound, i.e., $\mathscr{R}_h(u_h) \leq C\rho_h(u_h)$, where $C > 0$. This will be the subject of a further research.

2.3 Algebraic Residuum Estimators

Similarly as in the previous section, we define the estimator corresponding to the *algebraic error residuum*. Let $\tilde{u}_h \in S_{hp}$ be the output of the iterative process used for the solution of (6). We define the *algebraic residuum estimator*

$$\rho_h^A(\tilde{u}_h) := \sup_{0 \neq \psi_h \in S_{hp}} \frac{\tilde{c}_h(\tilde{u}_h, \psi_h)}{\|\psi_h\|_X} = \sup_{\psi_h \in S_{hp}, \|\psi_h\|_X = 1} \tilde{c}_h(u_h, \psi_h), \tag{16}$$

which measures the algebraic error (the difference between $\tilde{u}_h$ and u_h), since $\rho_h^A(u_h) = 0$ due to (6). The relations (14) and (16) give $\rho_h^A(\tilde{u}_h) \leq \rho_h(\tilde{u}_h)$, since in (14) the supremum is taken over the larger space.

We stop the iterative process for the solution of the nonlinear algebraic problem (6) if

$$\rho_h^A(\tilde{u}_h) \leq \beta \rho_h(\tilde{u}_h), \tag{17}$$

where $\beta \in (0,1)$. In numerical experiments we put $\beta \approx 0.01$.

2.4 Choice of the Norm $\|\cdot\|_X$

In order to ensure a fast evaluation of estimators ρ_h and ρ_h^A, we need to choose the norm $\|\cdot\|_X$ in a suitable way. We employ

$$\|\cdot\|_X := \left(\delta \|\cdot\|_{L^2(\Omega)}^2 + \varepsilon |\cdot|_{H^1(\Omega, \mathscr{T}_h)}^2\right)^{1/2}, \tag{18}$$

which guarantees that

$$\rho_h(u_h)^2 = \sum_{K \in \mathscr{T}_h} \rho_{h,K}(u_h)^2. \tag{19}$$

Here δ and ε denote the size of "convection" and "diffusion", respectively.

Therefore, it is sufficient to evaluate the element residuum estimators $\rho_{h,K}$, $K \in \mathscr{T}_h$. This is a standard task of seeking a constrain extrema over $S_K^{p_K+1}$ with the constraint $\|\psi_h\|_X = 1$. This can be done directly very fast since the dimension of $S_K^{p_K+1}$, $K \in \mathscr{T}_h$ is small.

2.5 Residuum-Nonconformity Estimators

We have already mentioned that the second building block of the error measure is given by the nonconformity $\mathscr{N}_h(u_h)$ defined by (7). For the purpose of a mesh adaptation, we define its local variant

$$\mathscr{N}_{h,K}(v) := \left(\sum_{\Gamma \in \mathscr{F}_h^I \cap \partial K} \int_\Gamma h_\Gamma^{-1} [\![v]\!]^2 \,\mathrm{d}S + \sum_{\Gamma \in \mathscr{F}_h^D \cap \partial K} \int_\Gamma h_\Gamma^{-1} (v - u_D)^2 \,\mathrm{d}S \right)^{1/2}, \quad v \in H^1(\Omega, \mathscr{T}_h). \tag{20}$$

Obviously, from (7) and (20), we have $\mathscr{N}_h(v)^2 = \sum_{K \in \mathscr{T}_h} \mathscr{N}_{h,K}(v)^2$. Finally, we define the *local* and *global residuum-nonconformity estimators* of the approximate solution $u_h \in S_{hp}$ by

$$\eta_{h,K}(u_h) := \left(\rho_{h,K}(u_h)^2 + \mathscr{N}_{h,K}(u_h)^2\right)^{1/2}, \quad K \in \mathscr{T}_h, \tag{21a}$$

and

$$\eta_h(u_h) := \left(\rho_h(u_h)^2 + \mathscr{N}_h(u_h)^2\right)^{1/2} = \left(\sum_{K \in \mathscr{T}_h} \eta_{h,K}(u_h)^2 \right)^{1/2}, \tag{21b}$$

respectively. In virtue of (10), (15) and (21), we expect that the global residuum-nonconformity estimator $\eta_h(u_h)$ approximates the error measure $\mathscr{E}_h(u_h)$. In the following we introduce an adaptation technique which produces a *hp*-mesh and the corresponding approximate solution such that the estimator $\eta_h(u_h)$ is under a given tolerance.

3 *hp*-Adaptation Process

In this section, we present a new *hp*-adaptive DG technique for the solution of (6). In Section 2, we defined the element and global residuum-nonconformity estimators $\eta_{h,K}$ and η_h, respectively. We employ the norm $\|\cdot\|_X$ given by (18) which guarantees that equality (19) is valid. As already mentioned, our interest is to find the solution $\tilde{u}_h \in S_{hp}$ such that

$$\eta_h(\tilde{u}_h) \le \omega, \tag{22}$$

where $\omega > 0$ is a given tolerance.

Let $\mathscr{T}_h$ be a given mesh and $\tilde{u}_h$ the corresponding approximation of (6). We require that

$$\eta_{h,K}(\tilde{u}_h) \le \frac{\omega}{\sqrt{\#\mathscr{T}_h}} \qquad \forall K \in \mathscr{T}_h, \tag{23}$$

where $\#\mathscr{T}_h$ denotes the number of elements of $\mathscr{T}_h$. Obviously, if (23) is satisfied then, due to (21b), condition (22) is valid and the adaptation process stops. Otherwise, we mark for refinement all $K \in \mathscr{T}_h$ violating (23).

Furthermore, all marked elements will be refined either by *h*- or by *p*-adaptation, namely, either we split a given mother element K into four daughter elements or we increase the degree of polynomial approximation for a given element. Thus the new mesh $\mathscr{T}_{\hat{h}}$ and new set $\{\hat{p}_K, K \in \mathscr{T}_{\hat{h}}\}$ are created. We interpolate the old solution on a new mesh and perform the next adaptation step till (22) is valid.

3.1 Regularity Indicator

The estimation of the regularity of the solution is an essential key of any *hp*-adaptation strategy. Our approach is based on a measure of inter-element jumps which is the base of the jump indicator from [5] and the shock capturing technique from [7].

We propose the *regularity indicator*

$$g_K(u_h) := \frac{\int_{\partial K\cap\Omega}[\![u_h]\!]^2\,\mathrm{d}S}{|K|h_K^{2p_K-2}}, \quad K\in\mathscr{T}_h, \tag{24}$$

where $|K|$ is the area of $K\in\mathscr{T}_h$. If the exact solution is sufficiently regular, i.e., $s_K \geq p_K+1$, then $g_K(u_h)\approx O\left(h_K^{2p_K+1}/h_K^2 h_K^{2p_K-2}\right) = O(h_K^1)$. On the other hand, if the exact solution is not sufficiently regular, i.e., $s_K < p_K+1$ ($\Leftrightarrow s_K \leq p_K$), then $g_K(u_h)\approx O\left(h_K^{2s_K-1}/h_K^2 h_K^{2p_K-2}\right) = O(h_K^{2\delta-1})$, where $\delta = s_K - p_k \leq 0$. Then we use the following strategy

$$\begin{array}{ll} g_K(u_h)\leq 1 & \Rightarrow \text{solution is regular} \quad \Rightarrow \text{p-refinement},\\ g_K(u_h)>1 & \Rightarrow \text{solution is irregular} \quad \Rightarrow \text{h-refinement}, \end{array} \qquad K\in\mathscr{T}_h. \tag{25}$$

4 Numerical Experiments

In the previous sections, we introduced and developed the adaptive *hp*-DGFE method. We demonstrate its performance in this section by several numerical examples. Let $\tilde{u}_h$ be the approximate solution resulting from an iterative method, i.e., the solution influenced by the algebraic error. We deal with two following numerical examples:

(E1) nonlinear convection-diffusion equation with a corner singularity from [9],

(E2) linear convection-diffusion equation with the strong interior layer and the exponential boundary layer from [10].

For the first one, we know the exact solution and therefore we are able to evaluate the computational error. We carried out a *hp*-adaptive algorithm starting on a mesh with the step h_0 and P_1 polynomial approximation. We evaluate $\|u-\tilde{u}_h\|_X$, $\mathscr{N}_h(\tilde{u}_h)$ and $\rho_h(\tilde{u}_h)$ with the corresponding experimental orders of convergence (EOC) with respect to the number of degree of freedom N_h defined by

$$\mathrm{EOC} = \frac{\log e_{h_{l+1}} - \log e_{h_l}}{\log(1/\sqrt{N_{h_{l+1}}}) - \log(1/\sqrt{N_{h_l}})}, \qquad l=1,2,\ldots, \tag{26}$$

Moreover, we evaluate the *"effectivity index"*

$$i_{\mathrm{eff}} := \frac{\eta_h(\tilde{u}_h)}{\left(\|u-\tilde{u}_h\|_X{}^2 + \mathscr{N}_h(\tilde{u}_h)^2\right)^{1/2}} = \frac{\left(\rho_h(\tilde{u}_h)^2 + \mathscr{N}_h(\tilde{u}_h)^2\right)^{1/2}}{\left(\|u-\tilde{u}_h\|_X{}^2 + \mathscr{N}_h(\tilde{u}_h)^2\right)^{1/2}}. \tag{27}$$

Let us note that the index i_{eff} is not a standard effectivity index since $\rho_h(\tilde{u}_h)$ is the approximation of $\mathscr{R}_h(\tilde{u}_h)$ and not of $\|u-\tilde{u}_h\|_X$. Obviously, if $\mathscr{N}_h(\tilde{u}_h)$ dominate $\rho_h(\tilde{u}_h)$ and $\|u-\tilde{u}_h\|_X$ then the index i_{eff} is close to one. In this case it would be also interesting to evaluate the ratio $\rho_h(\tilde{u}_h)/\|u-\tilde{u}_h\|_X$.

4.1 (E1): Nonlinear Convection-Diffusion Equation with a Corner Singularity

We consider the scalar nonlinear convection-diffusion equation

$$-\nabla\cdot(K(u)\nabla u) - \frac{\partial u^2}{\partial x_1} - \frac{\partial u^2}{\partial x_2} \;=\; g \quad \text{in } \Omega := (0,1)^2, \tag{28}$$

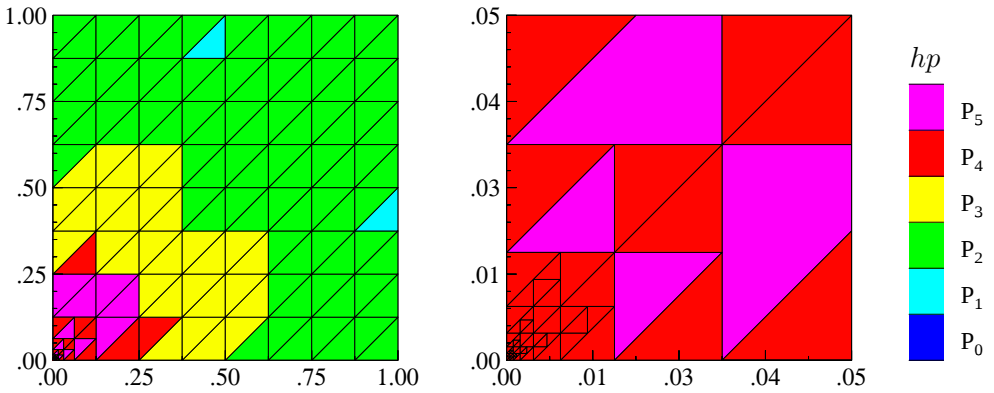

Source: Own

Fig. 1. *Example (E1) given by* (28) – (30) *with* $\alpha = -3/2$*: the final grid with the corresponding degrees of polynomial approximation, the whole domain (left) and its detail* $(0,1/20)\times(0,1/20)$ *(right)*

where $K(u)$ is the nonsymmetric matrix given by

$$K(u) = \varepsilon \begin{pmatrix} 2+\arctan(u) & (2-\arctan(u))/4 \\ 0 & (4+\arctan(u))/2 \end{pmatrix}. \tag{29}$$

The parameter $\varepsilon > 0$ plays a role of an amount of diffusivity and we put $\varepsilon = 10^{-3}$. We prescribe a Dirichlet boundary condition on $\partial\Omega$ and set the source term g such that the exact solution is

$$u(x_1,x_2) = (x_1^2+x_2^2)^{\alpha/2} x_1 x_2 (1-x_1)(1-x_2), \quad \alpha \in \mathbb{R}. \tag{30}$$

We present two choices: $\alpha = 4$ and $\alpha = -3/2$. It is possible to show (see [1]) that $u \in H^\kappa(\Omega)$, $\kappa \in (0, 3+\alpha)$, where $H^\kappa(\Omega)$ denotes the Sobolev-Slobodetskii space of functions with "non-integer derivatives". Whereas the choice $\alpha = 4$ gives sufficiently regular solution, the choice $\alpha = -3/2$ leads to the solution with a singularity at $x_1 = x_2 = 0$. Numerical examples presented in [4], carried out for a little different problem, show that this singularity avoids to achieve an order of convergence better than $O(h^{3/2})$ in the L^2-norm and $O(h^{1/2})$ in the H^1-seminorm for any degree of polynomial approximation. Nevertheless, the exact solution is regular outside of the singularity.

Table 1 shows the results for problem (28) – (30) with $\alpha = 4$ and $\alpha = -3/2$, namely the values of the error $\|u-\tilde{u}_h\|_X$, nonconformity $\mathscr{N}_h(\tilde{u}_h)$, residuum error estimate $\rho_h(\tilde{u}_h)$ with the corresponding EOC, index i_{eff} and the computational times in seconds. We observe that the computational error $\|u-\tilde{u}_h\|_X$ converge exponentially for $\alpha = 4$ and significantly faster than $O(h^{1/2})$ for $\alpha = -3/2$. Furthermore, the index i_{eff} is very close to one for increasing N_h which supports the accuracy of the method. A small increase of i_{eff} in Table 1 for $\alpha = 4$ for the last adaptation level is caused by the fact that we are close to the machine accuracy.

Furthermore, Figure 1 shows the final hp-grid obtained with the aid of the hp-DGFE algorithm for $\alpha = -3/2$. (The case $\alpha = 4$ is not interesting since only p-refinement is carried out due to the regularity of the exact solution.) We observe that the h-adaptation was carried out in a small region near the singularity. On the other hand, the p-adaptation appears in regions where the solution is regular.

Tab. 1. *Example (E1) given by* (28) – (30)*: error* $\|u-\tilde{u}_h\|_X$*, nonconformity* $\mathscr{N}_h(\tilde{u}_h)$*, residuum error estimate* $\rho_h(\tilde{u}_h)$ *with the corresponding EOC, index* i_{eff} *and the computational time in seconds*

$\alpha = 4$:

lev	$\#\mathscr{T}_h$	N_h	$\|u-\tilde{u}_h\|_X$	EOC	$\mathscr{N}_h(\tilde{u}_h)$	EOC	$\rho_h(\tilde{u}_h)$	EOC	i_{eff}	CPU(s)
0	128	384	6.45E-03	–	1.99E-02	–	5.58E-03	–	0.99	0.4
1	128	705	4.56E-04	8.72	3.07E-03	6.15	6.60E-04	7.03	1.01	0.7
2	128	384	6.45E-03	8.72	1.99E-02	6.15	5.58E-03	7.03	0.99	0.4
3	128	768	4.43E-04	7.73	3.01E-03	5.45	6.35E-04	6.27	1.01	0.7
4	128	1280	3.87E-05	9.54	2.75E-04	9.36	5.22E-05	9.78	1.01	1.0
5	128	1920	2.75E-06	13.05	1.73E-05	13.65	3.05E-06	14.02	1.00	1.4
6	128	2688	1.10E-07	19.12	7.04E-07	19.02	1.13E-07	19.59	1.00	2.2
7	128	3584	2.49E-09	26.35	1.62E-08	26.24	2.42E-09	26.72	1.00	3.4
8	128	4608	2.98E-11	35.22	2.23E-10	34.08	3.00E-11	34.92	1.00	5.3
9	128	5760	3.17E-15	82.03	2.02E-14	83.51	1.56E-14	67.83	1.25	9.0

$\alpha = -3/2$:

lev	$\#\mathscr{T}_h$	N_h	$\|u-\tilde{u}_h\|_X$	EOC	$\mathscr{N}_h(\tilde{u}_h)$	EOC	$\rho_h(\tilde{u}_h)$	EOC	i_{eff}	CPU(s)
0	128	384	1.32E-02	–	1.41E-01	–	4.52E-02	–	1.05	0.5
1	128	759	5.98E-03	2.32	6.70E-02	2.18	1.26E-02	3.75	1.01	0.8
2	128	919	5.50E-03	0.87	6.36E-02	0.55	6.26E-03	7.31	1.00	1.1
3	128	969	4.30E-03	9.31	5.52E-02	5.36	4.34E-03	13.81	1.00	1.4
4	134	1089	2.98E-03	6.29	3.96E-02	5.69	3.09E-03	5.86	1.00	1.6
5	140	1191	2.10E-03	7.81	2.75E-02	8.14	2.07E-03	8.91	1.00	1.9
6	152	1371	1.49E-03	4.82	1.93E-02	4.99	1.45E-03	5.03	1.00	2.1
7	158	1476	1.07E-03	9.07	1.37E-02	9.33	1.05E-03	8.72	1.00	2.5
8	164	1578	7.71E-04	9.78	9.78E-03	10.13	7.97E-04	8.34	1.00	2.9
9	176	1758	5.65E-04	5.75	7.04E-03	6.09	6.35E-04	4.21	1.00	3.3
10	188	1938	4.26E-04	5.81	5.15E-03	6.41	5.37E-04	3.43	1.00	3.8
11	200	2118	3.35E-04	5.41	3.87E-03	6.41	4.81E-04	2.48	1.00	4.3

Source: Own

4.2 (E2): Linear Convection-Diffusion Equation with the Strong Interior Layer and the Exponential Boundary Layer

We consider the example from [10], given by

$$-\varepsilon\triangle u + b_1\frac{\partial u}{\partial x_1} + b_2\frac{\partial u}{\partial x_2} = 0 \quad \text{in } \Omega := (0,1)^2, \tag{31}$$

where $\varepsilon = 10^{-8}$ is a constant diffusion coefficient and $(b_1,b_2) = (\cos(-\pi/3),\sin(-\pi/3))$ is the convection. We prescribe the Dirichlet boundary condition on $\partial\Omega$ by

$$u_D(x_1,x_2) = \begin{cases} 0 & \text{for } x_1 = 1 \text{ or } x_2 \le 0.7, \\ 1 & \text{otherwise.} \end{cases} \tag{32}$$

The solution possesses an interior layer in the direction of the convection starting in $(x_1,x_2) = (0,0.7)$ and contains two boundary layers along $x_1 = 0$ and $x_2 = 0$. On the boundary $x_1 = 1$ and on the right part of the boundary $x_2 = 0$, exponential layers are developed. The width of layers are proportional to ε.

For this case, the exact solution is piecewise constant except thin regions along the boundary and interior layer, however, its analytical expression is unknown. Therefore the computational

Tab. 2. *Example (E2) given by* (31) – (32) *with* $\varepsilon = 10^{-8}$*: the approximation of the error* $\|\overline{u} - \tilde{u}_h\|_X$*, nonconformity* $\mathcal{N}_h(\tilde{u}_h)$*, residuum error estimate* $\rho_h(\tilde{u}_h)$ *with the corresponding EOC, index* i_{eff} *and the computational time in seconds*

lev	$\#\mathcal{T}_h$	N_h	$\|\overline{u} - \tilde{u}_h\|_X$	EOC	$\mathcal{N}_h(\tilde{u}_h)$	EOC	$\rho_h(\tilde{u}_h)$	EOC	i_{eff}	CPU(s)
0	128	384	1.25E-01	–	3.58E+00	–	1.03E+00	–	1.04	0.3
1	128	635	9.56E-02	1.08	3.57E+00	0.01	7.60E-01	1.20	1.02	0.6
2	167	1211	8.06E-02	0.53	5.03E+00	-1.06	7.60E-01	-0.00	1.01	1.0
3	245	1984	7.50E-02	0.30	7.09E+00	-1.39	5.85E-01	1.06	1.00	2.2
4	467	3921	6.35E-02	0.49	1.00E+01	-1.02	5.95E-01	-0.05	1.00	4.0
5	1025	9751	6.12E-02	0.08	1.42E+01	-0.76	6.89E-01	-0.32	1.00	9.4
6	2189	21663	4.51E-02	0.76	2.01E+01	-0.87	7.32E-01	-0.15	1.00	18.2
7	4910	54765	3.17E-02	0.76	2.84E+01	-0.75	6.75E-01	0.17	1.00	50.8
8	7733	106285	2.28E-02	0.99	2.86E+01	-0.02	5.38E-01	0.68	1.00	196.6
9	14240	221582	1.76E-02	0.71	2.86E+01	-0.00	5.20E-01	0.09	1.00	505.8
10	19103	310336	1.62E-02	0.50	2.86E+01	-0.00	5.16E-01	0.04	1.00	1046.7
11	17849	272175	1.61E-02	-0.05	2.86E+01	0.00	5.16E-01	-0.00	1.00	1163.8
12	17426	250641	1.61E-02	-0.01	2.86E+01	-0.00	5.16E-01	0.00	1.00	1226.7
13	17366	240586	1.61E-02	0.03	2.86E+01	-0.01	5.16E-01	0.00	1.00	1248.5
14	17288	236116	1.61E-02	-0.16	2.86E+01	0.02	5.16E-01	0.01	1.00	1290.4
15	17207	233366	1.61E-02	0.12	2.86E+01	-0.05	5.16E-01	0.01	1.00	1311.4

Source: Own

error $\|u - \tilde{u}_h\|_X$ is approximated by $\|\overline{u} - \tilde{u}_h\|_X$ where $\overline{u}$ is piecewise constant function corresponding to the exact solution of (31) in the limit with $\varepsilon \to 0$. (The boundary conditions have to be modified of course.)

Table 2 shows the results of computations (E2) for problem (31) – (32), namely the values of the approximation of the error $\|\overline{u} - \tilde{u}_h\|_X$, nonconformity $\mathcal{N}_h(\tilde{u}_h)$, residuum error estimate $\rho_h(\tilde{u}_h)$ with the corresponding EOC, index i_{eff} and the computational times in seconds. The value $\|\overline{u} - \tilde{u}_h\|_X$ does not tend to zero, probably due to the difference between the exact solution u and its approximation $\overline{u}$. Moreover, the nonconformity $\mathcal{N}_h(\tilde{u}_h)$ is high, it will decrease with an additional mesh adaptation, however, here we face a problem with a too high number of degree of freedom and the limits of our computer. It would be more efficient to apply an anisotropic mesh adaptation. Nevertheless, the results show that the presented hp-method works reasonably, both layers are well captured.

Furthermore, Figure 2 shows the final hp-grid obtained with the aid of the hp-DGFE algorithm after 5, 10 and 15 adaptive cycles. We observe that the h-adaptation was carried out in regions near both layers. In regions, where the solution is constant, the P_0 approximation is finally used. We also observe that the algorithm is able to decrease N_h when the thin layers are well localized. Finally, Figure 3 shows the detail of the diagonal cut $[0,0] \to [1,1]$ of the approximate solution after $l = 5$, $l = 10$ and $l = 15$ adaptation cycles.

Conclusion

We presented a hp-adaptive numerical method for the solution of the second order boundary value problem. This approach is based on a heuristic approximation of the error measured in a dual norm. Although a theoretical justification of this technique is missing, numerical experiments show reasonable computational properties.

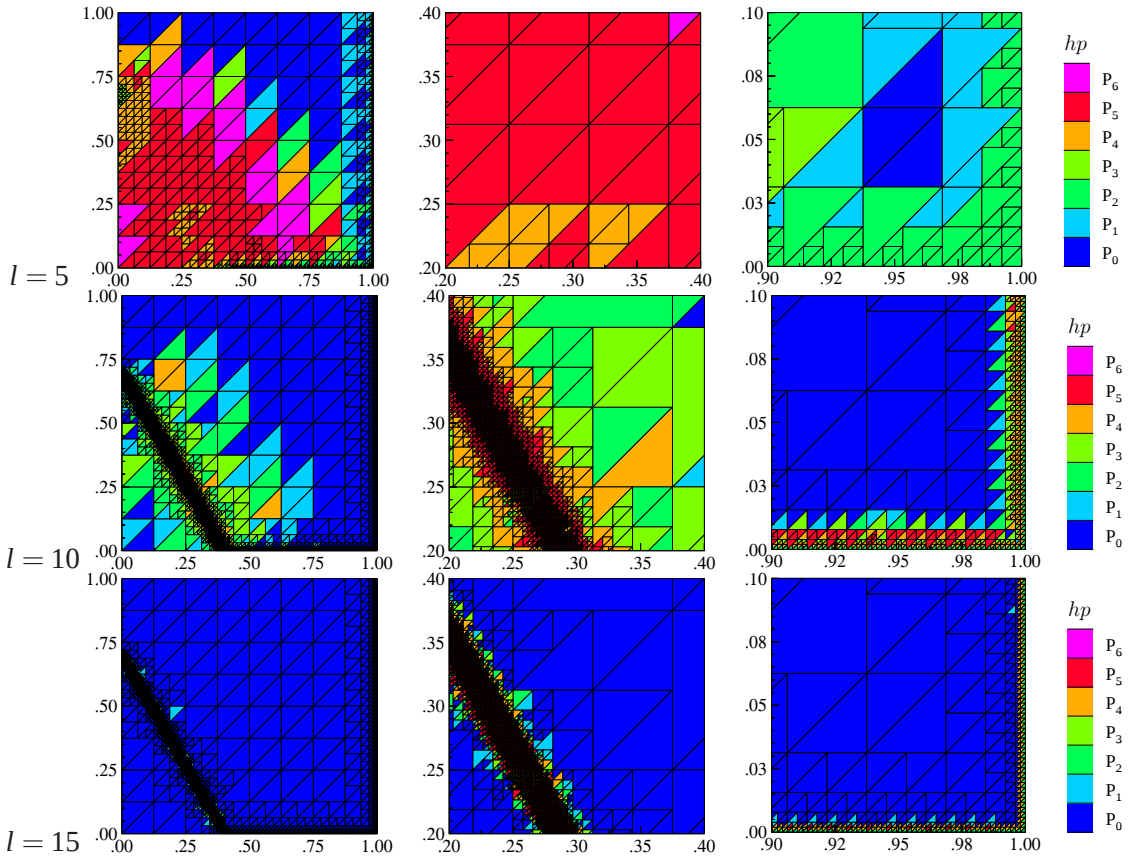

Source: Own

Fig. 2. *Example (E2) given by* (31) – (32) *with* $\varepsilon = 10^{-8}$*: the grids after* $l = 5, 10, 15$ *adaptation cycles with the corresponding degrees of polynomial approximation, the whole domain (left) and its details* $(0.2, 0.4) \times (0.2, 0.4)$ *(centre) and* $(0.9, 1) \times (0, 0.1)$ *(right)*

Acknowledgments

This work is a part of the research project Grant No. 201/08/0012 of the Czech Science Foundation.

Literature

[1] BABUŠKA, I.; SURI, M.: The *p*- and *hp*- versions of the finite element method. An overview. *Comput. Methods Appl. Mech. Eng.*, 80 (1990), pp. 5–26.

[2] BABUŠKA, I.; SURI, M.: The $p-$ and $hp-$FEM a survey. *SIAM Review*, 36 (1994), pp. 578–632.

[3] DOLEJŠÍ, V.; ERN, A.; VOHRALÍK, M.: A framework for robust a posteriori error control in unsteady nonlinear advection-diffusion problems. *SIAM J. Numer. Anal.*, (submitted for publication).

[4] DOLEJŠÍ, V.; FEISTAUER, M.; KUČERA, V.; SOBOTÍKOVÁ, V.: An optimal $L^\infty(L^2)$-error estimate of the discontinuous Galerkin method for a nonlinear nonstationary convection-diffusion problem. *IMA J. Numer. Anal.*, 28 (2008), pp. 496–521.

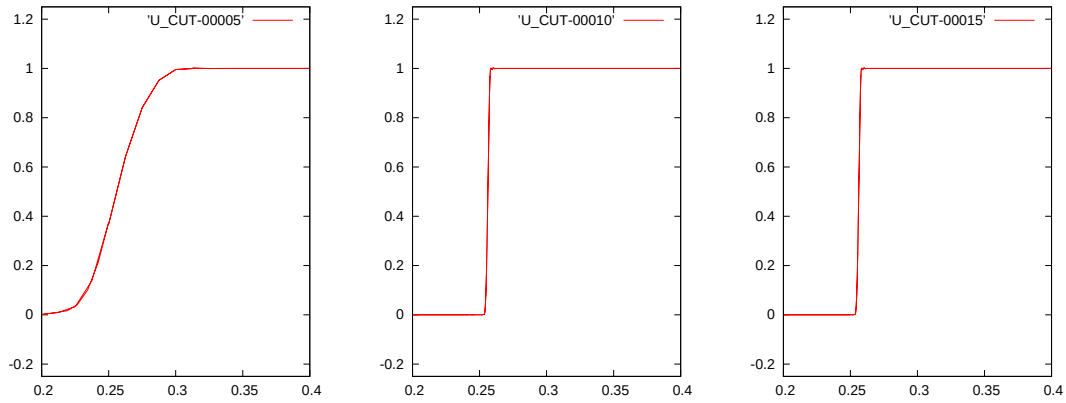

Source: Own

Fig. 3. *Example (E2) given by* (31) – (32) *with* $\varepsilon = 10^{-8}$*: detail of the diagonal cut* $[0,0] \to [1,1]$ *of the approximate solution* $l = 5$ *(left),* $l = 10$ *(centre) and* $l = 15$ *(right) adaptation cycles*

[5] DOLEJŠÍ, V.; FEISTAUER, M.; SCHWAB, C.: On some aspects of the discontinuous Galerkin finite element method for conservation laws. *Math. Comput. Simul.*, 61 (2003), pp. 333–346.

[6] EIBNER, T.; MELENK, J. M.: An adaptive strategy for *hp*-FEM based on testing for analyticity. *Comput. Mech.*, 39 (2007), pp. 575–595.

[7] FEISTAUER, M.; KUČERA, V.: On a robust discontinuous Galerkin technique for the solution of compressible flow. *J. Comput. Phys.*, 224 (2007), pp. 208–221.

[8] HOUSTON, P.; SÜLLI, E.: A note on the design of *hp*–adaptive finite element methods for elliptic partial differential equations. *Comput. Methods Appl. Mech. Engrg.*, 194 (2005), pp. 229–243.

[9] HOZMAN, J.: *Discontinuous Galerkin Method for Convection-Diffusion Problems*. PhD thesis, Charles University Prague, Faculty of Mathematics and Physics, 2009.

[10] JOHN, V.; KNOBLOCH, P.: On spurious oscillations at layer diminishing (SOLD) methods for convection–diffusion equations: Part I – A review. *Comput. Methods Appl. Mech Engrg.*, 196 (2007), pp. 2197–2215.

[11] KROLL, N.; BIELER, H.; DECONINCK, H.; COUALLIER, V.; VAN DER VEN, H.; SORENSEN, K., eds.: *ADIGMA A European Initiative on the Development of Adaptive Higher-Order Variational Methods for Aerospace Applications*. vol. 113 of Notes on Numerical Fluid Mechanics and Multidisciplinary Design, Springer Verlag, 2010.

[12] SCHWAB, C.: *p- and hp-Finite Element Methods*, Clarendon Press, Oxford, 1998.

[13] ŠOLÍN, P.; DEMKOWICZ, L.: Goal-oriented *hp*-adaptivity for elliptic problems. *Comput. Methods Appl. Mech. Engrg.*, 193 (2004), pp. 449–468.

prof. RNDr. Vít Dolejší, Ph.D., DSc.

hp-NESPOJITÁ GALERKINOVA METODA PRO NELINEÁRNÍ PROBLÉMY

Zabýváme se numerickým řešením nelineárních konvektivně-difusních rovnic pomocí nespojité Galerkinovy metody. Navrhujeme novou *hp*-adaptivní metodu, která je založena na residuálně-nekonformním odhadu chybu a indikátoru regularity řešení. Residuálně-nekonformní odhad se skládá ze dvou částí, residuálním odhadu chyby a tzv. hodnotě nekonformity. Pomocí odhadu chyby hledáme elementy sítě, které se mají zjemnit a indikátor regularity rozhoduje, zda-li mají být označené elementy zjemněny technikou *h* nebo *p*. Residuálně-nekonformní odhad a i indikátor regularity jsou snadno spočitatelné veličiny. Stejná technika může rovněž pomoci odhadnout chybu vzniklou z nepřesného řešení příslušné nelineární algebraické soustavy rovnic. Možnosti metody jsou dokumentovány pomocí několika numerických experimentů.

DIE *hp*-DISKONTINUIERLICHE GALERKIN-METHODE FÜR NICHTLINEARE PROBLEME

Wir beschäftigen uns mit de numerischen Lösung nichtlinearer konvektiv-diffuser Gleichungen mit Hilfe der diskontinuierlichen Galerkin-Methode. Wir entwerfen eine neue *hp*-adaptive Methode, die auf einer Kombination einer residual-nichtkonformen Fehlerschätzung und einem Regularitätsindikator beruht. Die residual-nichtkonforme Schätzung besteht aus zwei Teilen, der residualen Fehlerschätzung und dem so genannten Nichtkonformitätswert. Mit Hilfe der Fehlerschätzung suchen wir Netzelemente, die verfeinert werden sollen, und der Regularitätsindikator entscheidet, ob die bezeichneten Elemente mit der Technik *h* oder *p* verfeinert werden sollen. Die residual-nichtkonforme Schätzung und auch der Regularitätsindikator sind wohl berechenbare Größen. Die gleiche Technik kann ebenfalls bei der Schätzung eines Fehlers helfen, der aus einer ungenauen Lösung des zugehörigen nichtlinearen algebraischen Gleichungssystems hervorgegangen ist. Die Möglichkeiten der Methode werden mit Hilfe einiger numerischer Experimente dokumentiert.

hp-NIECIĄGŁA METODA GALERKINA DLA PROBLEMÓW NIELINIOWYCH

Zajmujemy się numerycznym rozwiązywaniem nieliniowych równań konwekcyjno-dyfuzyjnych przy pomocy nieciągłej metody Galerkina. Proponujemy nową metodę *hp*-adaptacyjną, opartą na rezydualnie niekonformicznym szacunku błędu i wskaźniku regularności rozwiązania. Szacunek rezydualno niekonformiczny składa się z dwóch części, rezydualnym szacunku błędu oraz tzw. wartości niezgodności. Za pomocą szacunku błędu poszukujemy elementów sieci, które mają zostać złagodzone a wskaźnik regularności decyduje o tym, czy zaznaczone elementy mają być złagodzone przy pomocy techniki *h* czy *p*. Szacunek rezydualno- niekonformiczny oraz wskaźnik regularności są wielkościami łatwymi do wyliczenia. Ta sama technika może pomóc także przy szacowaniu błędu powstałego w wyniku niedokładnego rozwiązania danego nieliniowego algebraicznego układu równań. Możliwości metody pokazano na przykładzie kilku eksperymentów numerycznych.